Pelvic Floor Dysfunction: Assessment with Combined Analysis of Static and Dynamic MR Imaging Findings[1]

Rania F. El Sayed, MD
Sahar El Mashed, MD
Ahmed Farag, MD
Medhat M. Morsy, MD
Mohamed S. Abdel Azim, MD

Purpose: To prospectively analyze static and dynamic magnetic resonance (MR) images simultaneously to determine whether stress urinary incontinence (SUI), pelvic organ prolapse (POP), and anal incontinence are associated with specific pelvic floor abnormalities.

Materials and Methods: This study had institutional review board approval, and informed consent was obtained from all participants. There were 59 women: 15 nulliparous study control women (mean age, 25.6 years) and 44 patients (mean age, 43.4 years), who were divided into four groups according to chief symptom. Static T2-weighted turbo spin-echo images were used in evaluating structural derangements; functional dynamic (cine) balanced fast-field echo images were used in detecting functional abnormalities and recording five measurements of supporting structures. Findings on both types of MR images were analyzed together to determine the predominant defect. Analysis of variance and the Bonferroni *t* test were used to compare groups.

Results: In the four patient groups, POP was associated with levator muscle weakness in 16 (47%) of 34 patients, with level I and II fascial defects in seven (21%) of 34 patients, and with both defects in 11 (32%) of 34 patients. SUI was associated with defects of the urethral supporting structures in 25 (86%) of 29 patients but was not associated with bladder neck descent. Levator muscle weakness may lead to anal incontinence in the absence of anal sphincter defects. Measurements of supporting structures were significant ($P < .05$) in the identification of pelvic floor laxity.

Conclusion: Combined analysis of static and dynamic MR images of patients with pelvic floor dysfunction allowed identification of certain structural abnormalities with specific dysfunctions.

[1] From the Departments of Radiology (R.F.E.S., S.E.M.), Surgery (A.F.), Anatomy (M.M.M.), and Urology (M.S.A.A.), Faculty of Medicine, Cairo University, Kaser El Aini Street, Cairo, Egypt 11511. Received June 28, 2007; revision requested August 31; revision received December 10; accepted January 21, 2008; final version accepted March 3. **Address correspondence to** R.F.E.S. (e-mail: *rania729@internetegypt.com*).

Female pelvic floor dysfunction is a general term applied to a wide variety of clinical conditions, most commonly stress urinary incontinence (SUI), pelvic organ prolapse (POP), and anal incontinence (1).

Static magnetic resonance (MR) imaging is utilized to delineate components of the pelvic organ support system, including the anal sphincter complex (2–9). Dynamic (cine) MR imaging with fast sequences enables functional evaluation to assess pelvic floor relaxation and pelvic organ descent (10–16). However, the precise anatomic causes of POP and SUI remain somewhat unclear. POP has been attributed both to damage to the levator ani muscle (10) and to an endopelvic fascial defect (17); however, some believe that it is still unclear which of these factors is more responsible (18–20). Similarly, SUI has been attributed to urethral hypermobility (21,22), to unequal movement of the urethral walls (23), and to defects in the urethral supporting structures (6,5,24,25).

Because of these controversies, treatment is often started regardless of the specific anatomic lesion involved. A report from Olsen et al (26) indicated that 29% of the procedures performed for incontinence and prolapse are repeat surgeries, suggesting the need for advances in both diagnosis and management of these disorders. DeLancey (27) emphasized the need for specific tests to pinpoint the specific anatomic defect responsible for pelvic floor dysfunction in each patient.

Thus, the purpose of our study was to prospectively analyze static and dynamic MR images simultaneously to determine whether SUI, POP, and anal incontinence are associated with specific pelvic floor abnormalities.

Advances in Knowledge

- Combined analysis of static and dynamic MR images of the pelvic floor reveals that certain anatomic defects on static images are associated with specific functional abnormalities on dynamic images.
- It is possible to differentiate whether prolapse is due to defects in the endopelvic fascia, to levator muscle weakness, or to abnormalities in both fascia and muscles.
- Stress urinary incontinence is associated with structural defects in the urethral supporting structures rather than with bladder neck descent.
- In the absence of an anal sphincter defect, anal incontinence is associated with marked levator muscle weakness.

Implication for Patient Care

- The association between precise anatomic defects in the pelvic organ support system and specific pelvic floor dysfunction allows a defect-specific approach to pelvic floor dysfunction for each patient.

Materials and Methods

Patients

The study group consisted of 59 women: 15 volunteer nulliparous women with a mean age of 25.6 years (range, 22–35 years), who served as a control group, and 44 women with a mean age of 43.4 years (range, 18–62 years), a parity range of 0 to 7, and clinical symptoms of pelvic floor dysfunction. The volunteers were employees of our institution who were recruited during the study period and who did not have lower genitourinary tract symptoms. The women with pelvic floor dysfunction symptoms presented consecutively between January 2004 and January 2005 to the clinicians involved in our study and were referred to a radiologist (R.F.E.S.) for assessment. The study was approved by our institution's review board, and informed consent was obtained from all participants. All volunteers and patients underwent both clinical examination and MR imaging.

The control group was subdivided into two subgroups, volunteer subgroup A and volunteer subgroup B, according to their MR imaging findings. MR images for volunteer subgroup A ($n = 9$) showed neither anatomic defects nor pelvic organ descent. In contrast, MR images for volunteer subgroup B ($n = 6$) demonstrated both anatomic defects and pelvic organ descent below the pubococcygeal line (PCL).

Patients were classified into one of four groups, depending on their chief symptom: POP without SUI (group A, $n = 10$), SUI without POP (group B, $n = 10$), SUI with bladder and/or genital prolapse (group C, $n = 16$), and anal incontinence associated with POP (group D, $n = 8$). Three of the eight patients in group D reported SUI in addition to their main disorder. Among the members of the four patient groups, five had undergone prior pelvic or anorectal surgery. Four patients had undergone various procedures for SUI: two patients from group A and one patient from group C had undergone transvaginal taping, one patient from group D had undergone bladder neck suspension, and one patient from group D had had undergone hemorrhoidectomy.

Clinical Examination

All control group members were interviewed and were found to be healthy, with no symptoms of lower genitourinary abnormalities, by using a validated questionnaire (28).

A urogynecologist (M.S.A.A., with 15 years of experience in clinical evaluation and management of pelvic floor dysfunction) examined the patients in groups A, B, and C, and a coloproctologist (A.F.,

Published online before print
10.1148/radiol.2482070974

Radiology 2008; 248:518–530

Abbreviations:
PCL = pubococcygeal line
POP = pelvic organ prolapse
SUI = stress urinary incontinence

Author contributions:
Guarantors of integrity of entire study, R.F.E.S., S.E.M., M.S.A.A.; study concepts/study design or data acquisition or data analysis/interpretation, all authors; manuscript drafting or manuscript revision for important intellectual content, all authors; manuscript final version approval, all authors; literature research, R.F.E.S., M.M.M.; clinical studies, R.F.E.S., A.F., M.S.A.A.; statistical analysis, R.F.E.S.; and manuscript editing, all authors

Authors stated no financial relationship to disclose.

with 19 years of experience) examined patients in group D and documented symptoms and physical findings. During pelvic examination, the Valsalva maneuver was performed, and the results of the clinical urinary stress test, as well as the degree and type of prolapse, were recorded and graded as follows: grade 0 indicated normal findings; grade I, minimal descent; grade II, descent halfway to the introitus; grade III, descent to the introitus; and grade IV, descent beyond the introitus (29). Clinical severity of anal incontinence was assessed by using the Pescatori score for anal incontinence (30). Anal sphincter tone, anal sphincter defects, levator ani tenderness, and defects and degree of relaxation of the puborectalis muscle were assessed with rectal examination (31).

MR Imaging

MR imaging was performed with the patient supine in a 1.5-T MR imaging unit (Gyroscan PowerTrak 6000; Philips Medical Systems, Best, the Netherlands) by using a pelvic phased-array coil. No oral or intravenous contrast agent was administered. All patients had undergone a rectal enema with warm water the night before the MR imaging examination and were asked to void 2 hours before the examination. The rectum was opacified with 90–120 mL of ultrasonographic gel (Aquasonic; Parker Laboratories, Fairfield, NJ) in all but eight patients, who either had a painful perianal condition (three patients had perianal fissures, and one had an acute attack of hemorrhoids) or refused the instillation of gel (four patients). The MR images of these patients were still of diagnostic quality; comment on rectocele was included in our report in five of these eight patients in

Figure 1

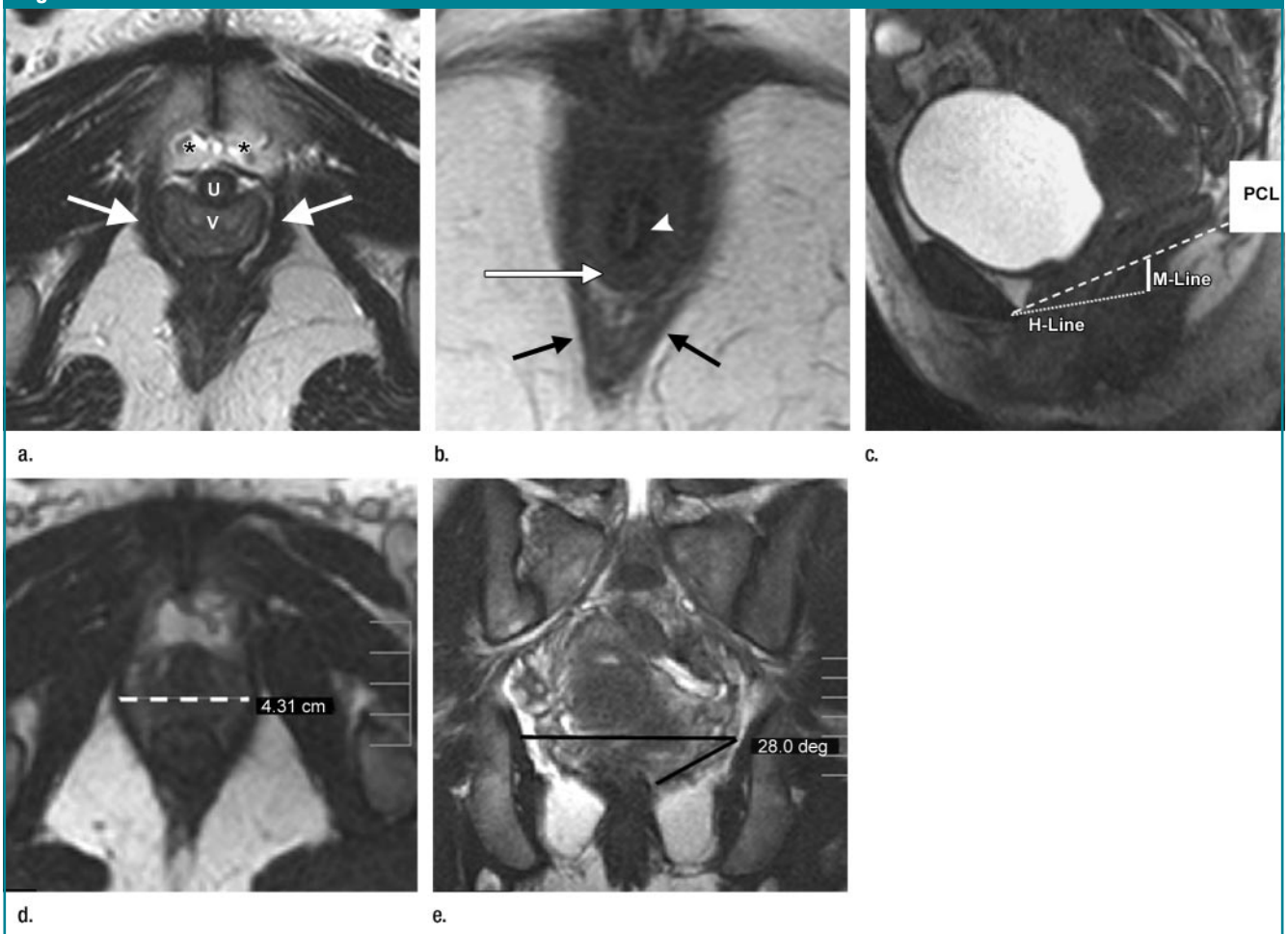

Figure 1: Normal static and dynamic MR imaging findings in 20-year-old woman in control group. **(a)** Axial T2-weighted turbo spin-echo image (5000/132) at level of proximal urethra *(U)* shows normal urethral supporting structures. Arrows = puborectalis slings, ∗ = space of Retzius, *V* = vagina. **(b)** Axial balanced fast-field echo image (9/4) of anal sphincter. The consecutive layers from the lumen outward include the innermost high-signal-intensity layer (the combined mucosa and submucosa), the low-signal-intensity layer (the submucosal smooth muscle [arrowhead]), the internal anal sphincter (white arrow), and the deep external anal sphincter (black arrows). **(c–e)** Dynamic **(c)** sagittal, **(d)** axial, and **(e)** coronal balanced fast-field echo MR images (5/1.6) obtained at maximum straining. In **c**, there is no POP; the H-line and the M-line are illustrated. In **d**, the width of the levator hiatus corresponds to the dashed line. In **e**, there is no excessive increase of the iliococcygeus angle (plotted lines).

whom the rectum was clearly delineated by air.

Static images of the pelvis were first acquired in three planes by using T2-weighted turbo spin-echo sequences (repetition time msec/echo time msec, 5000/132; field of view, 240–260 mm; section thickness, 5 mm; gap, 0.7 mm; number of signals acquired, two; flip angle, 90°; matrix, 512 × 512; acquisition time, 3.12 minutes for each sequence). In addition, T2-weighted balanced fast-field echo images (9.0/4.0; field of view, 220 mm; section thickness, 3 mm; number of signals acquired, eight; flip angle, 45°; matrix, 512 × 512; acquisition time, 2.12 minutes) of the anal sphincter complex were obtained in the control group volunteers and in patients in group D. In this sequence, section orientation was parallel and perpendicular to the plane of the anal canal (8,9).

Dynamic MR imaging was performed in the sagittal, axial, and coronal planes by using the balanced fast-field echo sequence (5.0/1.6; field of view, 300 mm; section thickness, 6–7 mm; gap, 0.7 mm). As a modification of a previous technique (14), in each plane we acquired five sections during six phases; each phase took 10 seconds. These six phases were acquired *(a)* with the patient at rest, *(b)* during contraction of the pelvic floor (the patient was instructed to squeeze the buttocks as if trying to prevent the escape of urine), *(c)* during mild straining, *(d)* during moderate straining, *(e)* during maximum straining, and *(f)* during a repeated maximum straining sequence to ensure a maximal Valsalva maneuver (the patient was instructed to bear down as much as she could, as though she were constipated and trying to defecate).

All participants were trained regarding these instructions before going to the MR imaging examination. A radiologist (R.F.E.S.) attended each MR imaging examination to ensure the compliance of the woman's response by observing the movement of the anterior abdominal wall, as well as the movement of the pelvic organs, to minimize variations between examinations.

Data Analysis

The MR imaging data sets were assessed by a radiologist (R.F.E.S., with 7 years of experience interpreting pelvic floor MR images). The radiologist was aware of each patient's clinical history and diagnosis. All measurements were obtained with software (DicomWorks, version 1.3.5; *http://dicom.online.fr/*). A consensus reading of the MR images for patients in groups A, B, and C was performed by the radiologist (R.F.E.S.) and the urogynecologist (M.S.A.A.),

Figure 2

A. Location and type of prolapse:

1. Anterior compartment:
   a. Bladder neck descent; grade: _____
   b. Bladder base descent; grade: _____

2. Middle compartment:
   a. Uterine descent; grade: _____
   b. Enterocele/peritoneocele; grade: _____

3. Posterior compartment:
   a. Anorectal junction descent; grade: _____
   b. Rectocele; grade: _____

B. Defects in the pelvic supporting system:

1. Urethral supporting structures:
   a. Ligament(s); type of injury: _____; side: _____
   b. Fascia level III:
   c. Puborectalis; type of injury: _____; side: _____

2. Vaginal supporting structures:
   a. Vaginal fascia level I and II; side: _____
   b. Iliococcygeus; type of injury: _____; side: _____

C. Anal sphincter:

a. External anal sphincter; level of injury: _____; site: _____; type of injury: _____
b. Internal anal sphincter; level of injury: _____; site: _____; type of injury: _____

D. Measurements of supporting structures :

H-Line: _____; M-line: _____; levator plate angle: _____
Width of levator hiatus: _____
Iliococcygeus angle: _____

Opinion

The predominant defect(s) is(are): _____
Ligaments: _____
Fascia: _____
Muscles injury and/or weakness: _____

Figure 2: Schematic presentation of MR imaging report.

and a consensus reading of the MR images for patients in group D was performed by the radiologist and the coloproctologist (A.F.).

Analysis of static MR images.—Analysis of static images in the control and patient groups was based on scrutiny of the urethral supporting system, the vaginal supporting system, and the anal sphincter complex.

The urethral supporting structures consist of ligaments (32), level III fascial support (18), and the puborectalis muscle (4). On images obtained in the axial plane, urethral ligament abnormalities were classified as distorted when internal architectural changes with waviness of the ligaments were seen and as a defect when there was discontinuity of the ligament with visualization of the torn parts (5,6). A level III fascial defect was recognized by the "drooping mustache sign," which is formed by fat in the prevesical space against the bilateral sagging of the detached lower third of the anterior vaginal wall from the arcus tendineus fascia (7). A puborectalis muscle defect was recognized by the loss of the normal symmetric appearance of the muscle slings or disruption of the attachment of the muscle to the pubic bone (4–6).

Vaginal supporting structures include level I fascia (which suspend the upper portion of the vagina from the pelvic wall), level II fascia (which attach the midportion of the vagina more directly to the pelvic wall) (19), and the iliococcygeus muscle. In the axial plane, a defect in the fascia was visualized as sagging of the fluid-filled posterior urinary bladder wall due to the detachment of the vaginal supporting fascia from the lateral pelvic wall, known as the "saddlebags sign" (7). The iliococcygeus muscle was assessed for loss of the normal symmetric appearance of its muscle slings or disruption of its attachment to the obturator internus muscle in the coronal plane.

For evaluation of the anal sphincter complex, the normal thickness of each muscle layer and the total thickness of the anal sphincter (measured from the inner border of the internal anal sphincter to the outer border of the external

Table 1

Findings Regarding Pelvic Organ Support System Defects on Static Axial MR Images in Control Group

	Urethral Supporting Structures			Vaginal Supporting Structures					
				Level I and II Vaginal Endopelvic Fascia					
Volunteer Subgroup	Ligaments	Level III Fascia	Puborectalis Muscle	Paravaginal	Central	Paravaginal and Central	Iliococcygeus Muscle	Anal Sphincter: External	Anal Sphincter: Internal
A ($n = 9$)	0	0	0	0	0	0	0	0	0
B ($n = 6$)	0	0	0	2	0	4	0	0	0

Note.—Data are numbers of volunteers with a defect in the given structure.

Figure 3

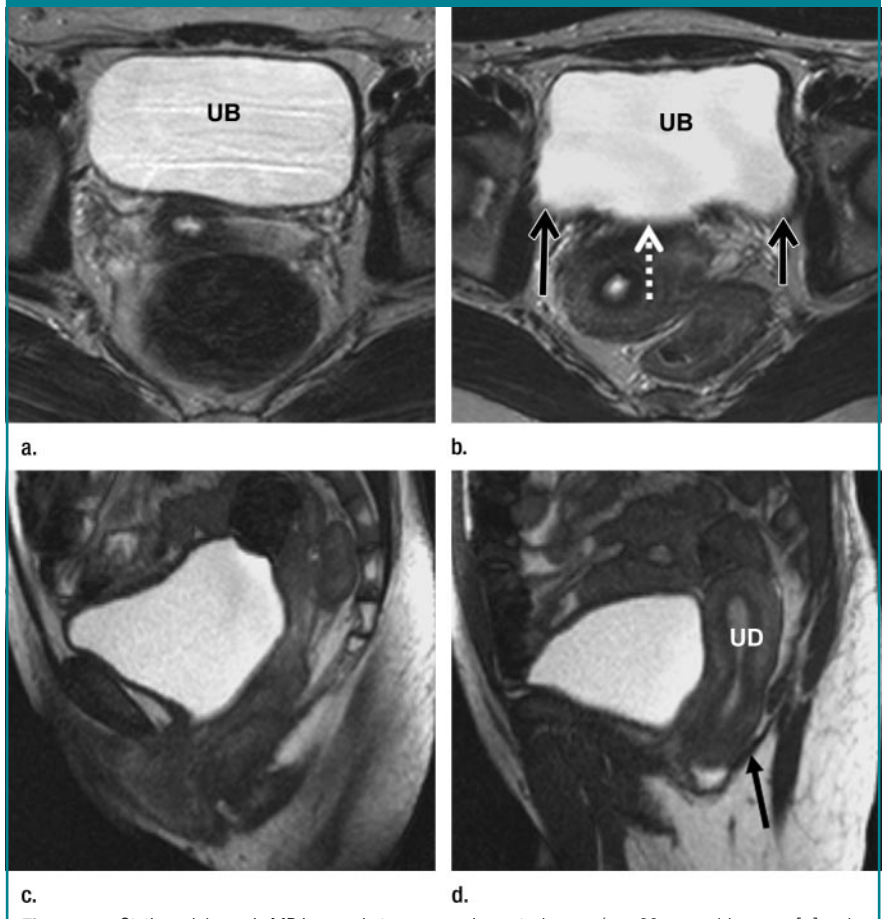

Figure 3: Static and dynamic MR images in two women in control group (one 20-year-old woman [**a**] and one 25-year-old woman [**b–d**]). **(a, b)** Static axial T2-weighted turbo spin-echo images (5000/132) show **(a)** normal level I vaginal fascial support, compared with **(b)** central (dashed arrow) and paravaginal (solid arrows) level I fascial defects. *UB* = urinary bladder. **(c)** Dynamic cine midsagittal and **(d)** parasagittal balanced fast-field echo MR images (5/1.6) obtained at maximum straining; **d** (obtained routinely within the five sections in each dynamic sequence) demonstrates uterine descent *(UD)* and the ileococcygeus muscle (arrow) better than **c** alone does.

anal sphincter) were measured in the control group. Anal sphincter lesions were classified according to the muscle injured (the internal or external anal sphincter or the puborectalis muscle) and according to lesion type (defect and/or scarring). A sphincteric defect was defined as discontinuity of the muscle ring; scarring was defined as a low-signal-intensity deformation of the normal pattern of the muscle layer (33).

Analysis of dynamic MR images.—In the sagittal plane, the PCL, which extends from the inferior border of the symphysis pubis anteriorly to the tip of the coccyx posteriorly, was used as the reference line. For each participant, the descent of the bladder neck, bladder base, uterus, and anorectal junction below the PCL (15) was recorded. In the patient groups, loss of urine through the urethra at maximum straining was also recorded. (However, absence of urine loss during MR imaging was not considered to invalidate the patient's report of SUI.)

Other measurements in the sagittal plane during maximum straining included the H-line, which extends from the inferior aspect of the pubic symphysis to the anorectal junction; the M-line, which drops as a perpendicular line from the PCL to the posterior aspect of the H-line (11); and the levator plate angle, which is enclosed between the levator plate and the PCL (12). In the axial and coronal planes, respectively, the width of the levator hiatus (14) and the iliococcygeus angle (2) were measured at rest and during maximum straining. These five measurements of supporting structures were all considered to reflect the status and the weakness of the levator ani (Fig 1).

Combined analysis of static and dynamic MR images.—Findings obtained from static and dynamic MR images in the same patient were then analyzed simultaneously to determine whether a particular anatomic defect detected on static images was associated with a specific dysfunction on dynamic images. The most marked type of pelvic supporting system defect was reported as the predominant defect (Fig 2).

Statistical Analysis

The mean and standard deviation of the measurements for the control subgroups and for each patient group were calculated.

The mean and standard deviation of the measurements of supporting struc-

Table 2

Findings Regarding Dysfunction and Measurements of Supporting Structures on Dynamic Cine MR Images in Control Group

Volunteer Subgroup	Pelvic Organ Descent (cm)*				H-Line (cm)*	M-Line (cm)*	Levator Plate Angle (degrees)*	Width of Levator Hiatus in Axial Plane (cm)		Ileococcygeus Angle in Coronal Plane (degrees)	
	Bladder Neck	Bladder Base	Uterus	Other†				At Rest	At Maximum Straining	At Rest	At Maximum Straining
A ($n = 9$)	No descent below PCL (9/9)	No descent below PCL (9/9)	No descent below PCL (9/9)	None (9/9)	5.8 ± 0.5	1.3 ± 0.5	11.7 ± 4.8	3.3 ± 0.4	4.5 ± 0.7	20.9 ± 3.5	33.4 ± 8.2
B ($n = 6$)	0.8 ± 0.4 (6/6)	0.9 ± 0.5 (6/6)	1.1 ± 0.2 (4/6)	None (6/6)	6.1 ± 0.8	1.9 ± 0.8	33 ± 12.9	3.1 ± 0.4	5.9 ± 1.3	24 ± 1.8	40.1 ± 8.6

Note.—No volunteer in the control group had SUI, defined as loss of urine at maximum straining, on dynamic cine MR images. Data are means ± standard deviations, with numbers in parentheses indicating in how many of the total number of volunteers mean pelvic organ descent was calculated.

* As measured in sagittal plane at maximum straining.

† Including peritoneocele, enterocele, rectocele, and anorectal junction descent.

Table 3

Findings Regarding Pelvic Organ Support System Defects on Static Axial MR Images in Patient Groups

Patient Group	Urethral Supporting Structures			Vaginal Supporting Structures					
				Level I and II Vaginal Endopelvic Fascia				Anal Sphincter	
	Ligament	Level III Fascia	Puborectalis Muscle	Paravaginal	Central	Paravaginal and Central	Iliococcygeus Muscle	External	Internal
A: POP only ($n = 10$)	0	0	0	6	1	2	1	0	0
B: SUI only ($n = 10$)	0	9	0	3	1	4	0	0	0
C: SUI and POP ($n = 16$)	4	8	1	9	1	6	0	1 (Thinning)	0
D: Anal incontinence and POP ($n = 8$)*	0	2	1	4	0	2	2	6 (Defects)†	3 (Scarring)

Note.—Data are numbers of patients with a defect in the given structure.

* Three of these patients also reported SUI in addition to their main disorder.

† Two patients had intact sphincters.

tures in volunteer subgroup A were compared with those in volunteer subgroup B and with those in patient groups by using software (InStat, version 3.05; GraphPad Software, San Diego, Calif). We used one-way analysis of variance to determine the statistical difference between these measurements. Whenever a measurement was shown to be statistically significant, we then used the Bonferroni *t* test to determine which group's measurements were statistically significant compared with those for volunteer subgroup A. Differences were considered significant at $P < .05$ and highly significant at $P < .001$.

Results

Combined Analysis of Static and Dynamic MR Images

Control group.—On static axial MR images, a central type of fascial defect was detected in combination with a paravaginal defect in four members of volunteer subgroup B (Table 1). This type of defect led to sagging of the midportion of the posterior wall of the urinary bladder (Fig 3).

Combined analysis of static and dynamic MR images in volunteer subgroup B (Tables 1 and 2) demonstrated that POP was mainly due to the presence of defects in level I and level II endopelvic fascia, because levator muscle weakness, as indicated by all measurements of supporting structures in this subgroup except the levator plate angle, was of no significant statistical difference from that in volunteer subgroup A.

The thicknesses of the muscle layers of the anal sphincter complex in the control group were as follows: external muscle layer, 2.07 mm ± 0.45 (standard deviation); internal muscle layer, 4.16 mm ± 0.72; and longitudinal muscle layer, 1.04 mm ± 0.4. The total thickness of the anal sphincter was 9.07 mm ± 2.59.

Patient group A.—In the patient group with POP but without SUI, POP was found to be related to a predominant fascial defect in three patients, to levator muscle weakness in two pa-

Table 4

Findings Regarding Dysfunction and Measurements of Supporting Structures on Dynamic Cine MR Images in Patient Groups

Patient Group	Pelvic Organ Descent (cm)*						Levator Plate Angle (degrees)*	Width of Levator Hiatus in Axial Plane (cm)		Iliococcygeus Angle in Coronal Plane (degrees)	
	Bladder Neck	Bladder Base	Uterus	Other†	H-Line (cm)*	M-Line (cm)*		At Rest	At Maximum Straining	At Rest	At Maximum Straining
A: POP only ($n = 10$)	1 ± 0.7 (7/10)	1.4 ± 1 (7/10)	3.1 ± 1 (6/10)	7	7 ± 0.7	2.9±1.2	40.6 ± 16.9	4.2 ± 0.6	7.2 ± 1.7	24 ± 1.8	57.95 ± 14
B: SUI only ($n = 10$)	0.6 ± 0.3 (5/10)	0.7 ± 0.4 (5/10)	No uterine descent	0	5.95 ± 0.7	2.4 ± 1.1	17.9 ± 1.1	3.2 ± 0.3	4.4 ± 0.8	25.1 ± 1.8	35.9 ± 9.2
C: SUI and POP ($n = 16$)	1.9 ± 0.5 (16/16)	2.3 ± 0.9 (16/16)	1.7 ± 0.7 (11/16)	4	7.9 ± 0.6	3.7 ± 1.1	50.5 ± 16.8	4.2 ± 0.5	7.4 ± 0.8	24.8 ± 20	61 ± 7
D: Anal incontinence and POP ($n = 8$)‡	2 ± 0.8 (8/8)	2.9 ± 1.2 (8/8)	4.1 ± 1.7 (8/8)	5	10.9 ± 1.9	5.98 ± 2.1	77.6 ± 18.9	4.5 ± 0.4	7.95 ± 0.8	27.5 ± 5.2	73.2 ± 10.4

Note.—No patient in group A, seven patients in group B, 12 patients in group C, and two patients in group D had SUI, defined as loss of urine at maximum straining, on dynamic cine MR images. Unless otherwise specified, data are means ± standard deviations, with numbers in parentheses indicating in how many of the total number of patients mean pelvic organ descent was calculated.

* As measured in sagittal plane at maximum straining.

† Including peritoneocele, enterocele, rectocele, and anorectal junction descent; data are numbers of patients with one or more of these other dysfunctions.

‡ Three of these patients also reported SUI in addition to their main disorder.

tients, and to both abnormalities in five patients (Tables 3, 4; Fig 4). Urinary loss did not accompany the bladder neck descent that was detected in seven patients; none of these patients reported SUI.

Patient group B.—In the patient group with SUI but without POP, level III fascial anatomic defects in the urethral supporting structures were detected in nine patients (Table 3). Dynamic sagittal images revealed a characteristic vertical direction of bladder neck movement (Fig 5). In one patient, no gross defects of urethral supporting structures were detected.

Patient group C.—In the patient group with SUI and bladder and/or genital prolapse, on static axial MR images, all patients were seen to have anatomic defects at the vaginal fascial levels. For the urethral supporting system, defects involving the muscular and ligamentous structures were detected in five of 16 patients (Fig 6), whereas eight of 16 patients had a level III fascial defect (Table 3). In three of 16 patients, atypical distortion of the ligaments and level III fascia was detected.

POP was due to a fascial defect in four patients, to levator muscle weakness in six patients, and to both defects in six patients. SUI was almost always associated with defects in one of the urethral supporting structures.

Patient group D.—In the patient group with anal incontinence and POP with or without SUI, on static MR images, structural defects of the anal sphincter were detected in six patients (Fig 7), three of whom also reported SUI. These three patients also had anatomic defects of the urethral supporting structures. On images obtained with dynamic sequences, there was marked levator muscle weakness (Table 4). Combined analysis of static and dynamic MR images suggested that marked levator muscle weakness was the main factor leading to POP in all patients in this group. This weakness was suggested as the cause of anal incontinence in the two patients who had no anal sphincter defects (Fig 8).

Figure 4

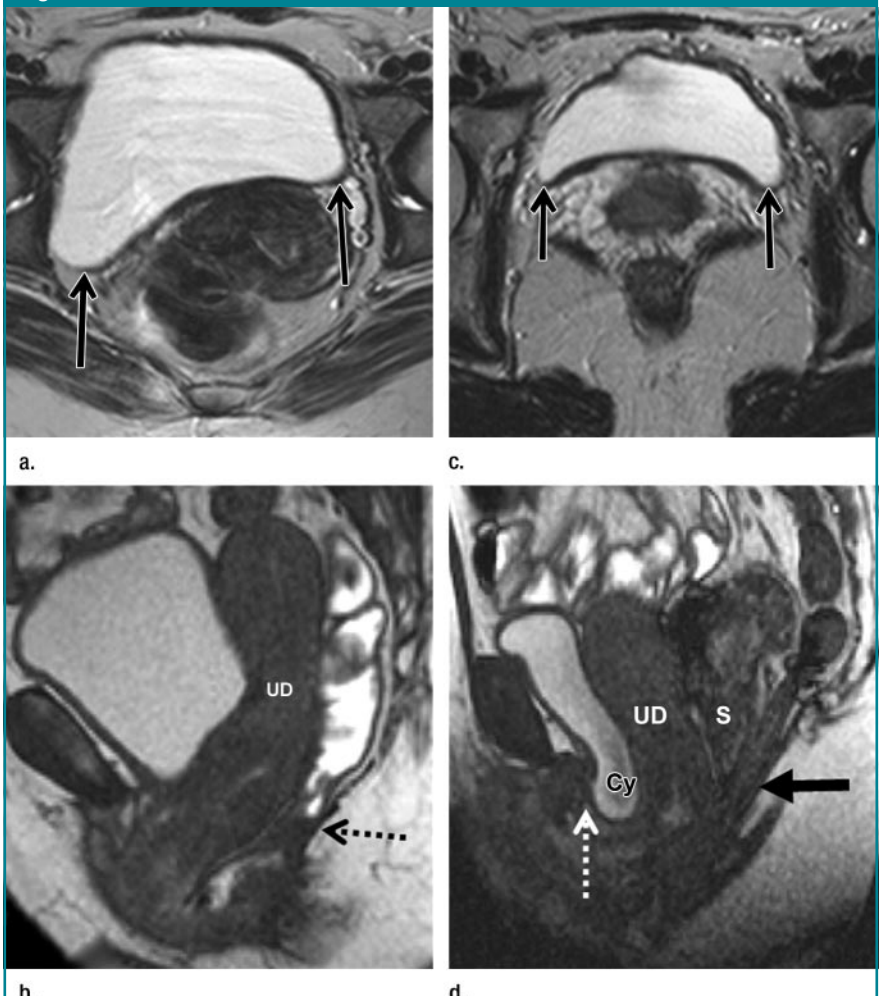

Figure 4: Static and dynamic MR images in two patients with POP (one 27-year-old woman [**a, b**] and one 54-year-old woman [**c, d**]). **(a, c)** Static axial T2-weighted turbo spin-echo images (5000/132). **(b, d)** Corresponding dynamic sagittal balanced fast-field echo images (5/1.6) at maximum straining. In **a**, a bilateral asymmetric level I paravaginal fascial defect (arrows) is more severe on the right. In **b**, a sagging levator plate (arrow) and uterine descent *(UD)* can be seen; combined analysis of static and dynamic imaging findings for this patient revealed a predominant fascial defect. In **c**, a bilateral symmetric level I paravaginal fascial defect (arrows) is seen. In **d**, bladder neck descent (dashed arrow), cystocele *(Cy)*, uterine descent *(UD)*, sigmoidocele *(S)*, and the excessive sagging of the levator plate (solid arrow) relative to the fascial defect indicate that levator muscle weakness is the predominant defect responsible for POP (this patient did not report SUI even after cystocele repair).

Statistical Analysis

The mean pelvic organ descent and the mean measurements of supporting structures in the control and patient groups (with standard deviations) are presented in Tables 1 and 2 and Tables 3 and 4, respectively.

Analysis of variance revealed that measurements of supporting structures were of highly significant difference ($P < .001$) between the six groups. Detailed values of t tests and the exact P values for each measured criterion of volunteer subgroup A versus other groups are presented in Tables 5 and 6. The differences in measurements of supporting structures between patient groups C and D were either significant ($P < .05$) or highly significant ($P <$

.001). Measurements for patient group A were also significantly different, except for the iliococcygeus angle at rest ($P = .056$). The measurements for volunteer subgroup B and for patient group B were not significantly different from those for volunteer subgroup A, except for the levator plate angle for volunteer subgroup B ($P = .0123$) and the iliococcygeus angle at rest for patient group B ($P = .004$) (Tables 5 and 6).

The frequency of defects and the most common predominant defects were as follows: In the four patient groups ($n = 44$), 34 patients reported POP, and levator muscle weakness was the predominant defect, being seen in 16 (47%) of 34 patients. Level I and II fascial defects were seen in seven (21%) of 34 patients, and both muscular and fascial defects were seen in 11 (32%) of 34 patients. Of the 29 women with SUI, 25 (86%) had an injury involving one of the urethral supporting structures. The most frequent injury was a level III fascial defect, detected in 19 (76%) of these 25 women.

Figure 5

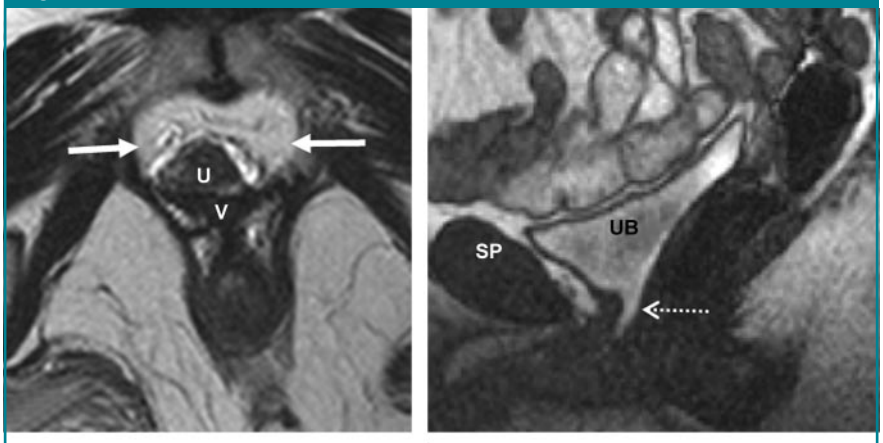

Figure 5: Static and dynamic MR images in 48-year-old patient with SUI. **(a)** Static axial T2-weighted turbo spin-echo image (5000/132) at level of proximal urethra shows a level III endopelvic fascial defect, indicated by the "drooping mustache" sign (arrows), misalignment of the urethra *(U)*, and distorted H-shaped vagina *(V)*. **(b)** Dynamic sagittal balanced fast-field echo image (5/1.6) shows loss of urine during straining; the bladder neck movement was noted to be in a vertical (arrow) and not rotational direction. This type of movement was frequently associated with level III endopelvic fascial defects. *SP* = symphysis pubis, *UB* = urinary bladder.

Discussion

In our study, we found a noteworthy relationship between static and dynamic MR imaging findings. This relationship provided insight into the association between MR imaging findings and pelvic floor symptoms.

In patients with POP, we were able to differentiate whether POP was due to endopelvic fascial defects, to marked levator muscle weakness, or to both by comparing volunteers in subgroup B and patients in group D. Static and dynamic MR images in volunteer subgroup B showed that POP was caused mainly by defects in level I and level II endopelvic fascia, as levator muscle weakness was mild in this control subgroup. In contrast, group D patients demonstrated a more advanced degree of muscle weakness relative to the fascial defect; these findings indicated that levator muscle weakness, rather than defects in the endopelvic fascia, was the main factor responsible for POP. The MR imaging findings in volunteer subgroup B also indicated that absence of symptoms is not necessarily associated with absence of structural defects or pelvic organ descent.

In previous work (10), POP has been attributed to damage to the levator muscle. DeLancey (18,19), however, described the interaction between pelvic floor muscles and endopelvic fascia and maintained that it was not possible to determine whether damage to muscle or damage to fascia is responsible for prolapse, because these two aspects of pelvic support are intimately interdependent.

Our results demonstrate that SUI is associated with the presence of defects in the urethral supporting structures. We found mainly level III endopelvic fascial defects on static MR images but no bladder neck hypermobility on dynamic MR images. These findings were supported by the fact that SUI was neither accompanied by bladder neck descent in seven patients in group A nor associated with the advanced degree of bladder neck descent encountered in group D. In addition, in the latter group, only the three patients who had SUI also had defects in the urethral supporting structures on static MR images. At the same time, the presence of defects in level I and level II endopelvic fascia in patients with SUI could not be considered a contributing factor to the patients' symptoms, because the existence of similar defects in volunteer subgroup B and in group A patients was not accompanied by SUI.

In agreement with our findings is the hammock hypothesis suggested by DeLancey (24), who reported that loss of level III endopelvic fascial support at the vesical neck is one of the factors responsible for SUI. Our findings demonstrate at imaging what had been hypothesized. Furthermore, in more recent studies (5,6), static MR imaging revealed a higher prevalence of lesions of the urethral supporting system in patients with SUI than in age-matched study control subjects.

In contrast to our findings, Klutke et al (3), who used static MR imaging, and others (14,16), who used dynamic MR imaging, have suggested urethral hypermobility as one of the causes of SUI. Yang et al (10), who used only dynamic MR imaging, did not resolve the paradoxical lack of urinary incontinence in some patients with large cystocele because they believed it was un-

clear whether the cause was kinking of the urethra or other factors.

In addition to pinpointing the underlying structural abnormality of these disorders, our approach has several clinical implications. In SUI, combined analysis of static and cine MR images revealed an association between level III fascial defects and vertical bladder neck movement. We believe that identification of a predominant anatomic defect on static images and its effect on the kinematics of the pelvic organ in dynamic sequences could be of value, making it possible in the future to use MR imaging to choose the most appropriate surgical technique from among the available therapeutic options for SUI (34,35). For POP, many types of cystocele are currently lumped under this single term and can be documented on sagittal dynamic MR images obtained at maximum straining. However, it is not possible from these midline images to see the specific differentiating structural defects (27). Therefore, instead of the clinician focusing on a "dropped bladder," combined analysis of both kinds of MR images can provide the clinician with complete mapping of the site and type of defects. Such information may help the clinician decide on physiotherapy for a patient with global muscle weakness and normal fascia but on surgical repair for a patient with a focal break in the fascia and/or a muscle tear. Thus, the suggested approach allows integration of static and dynamic MR imaging findings so that clinicians can more precisely identify the underlying anatomic defect responsible for symptoms in individual patients with pelvic floor dysfunction (even allowing differentiation of the underlying anatomic defect when any two patients have the same symptoms) and can thus decide on a more tailored treatment of the underlying abnormality.

Figure 6

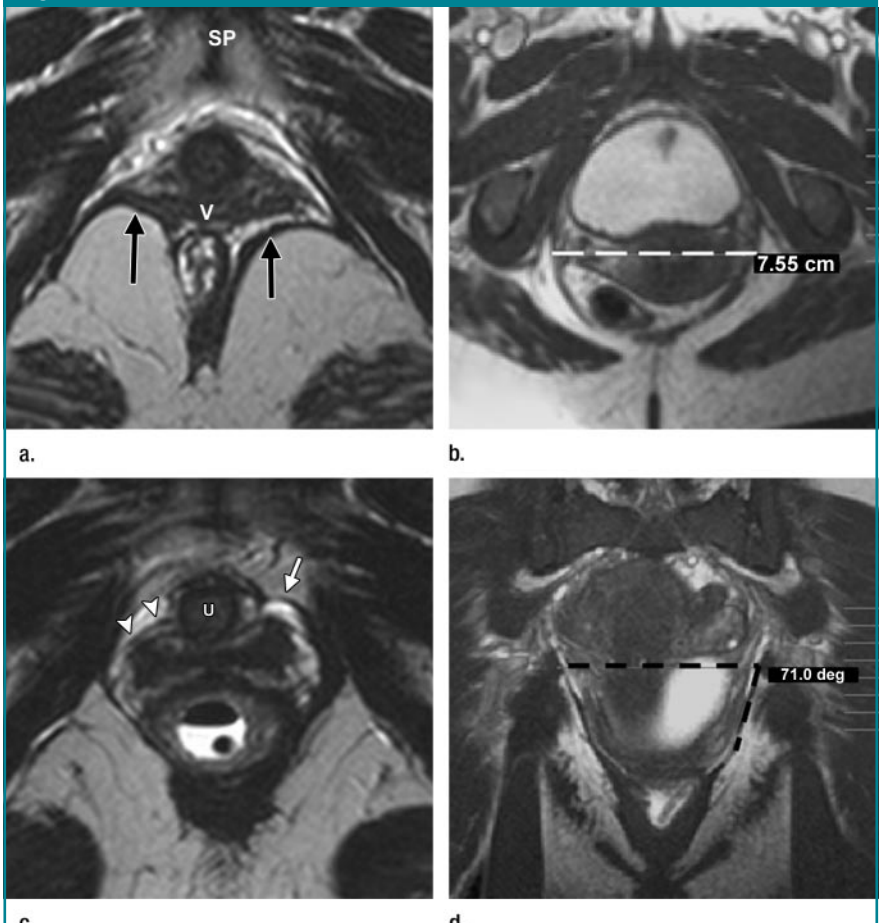

Figure 6: Static and dynamic MR images in two patients (one 49-year-old woman [**a, b**] and one 42-year-old woman [**c, d**]) with both SUI and POP. **(a)** Static axial T2-weighted turbo spin-echo image (5000/132) of proximal urethra shows muscular defect, reflected by detachment of the puborectalis muscle (arrows) from the pubic bone on both sides. *SP* = symphysis pubis, *V* = vagina. **(b)** Dynamic axial balanced fast-field echo image (5/1.6) at maximum straining shows width of levator hiatus to be 7.55 cm (dashed line). **(c)** Static axial T2-weighted image obtained with same sequence as **a** shows distortion of periurethral ligaments (arrowheads) on the right side, with the ligament receding backward compared with the normal left side (arrow). *U* = urethra. **(d)** Dynamic coronal image at maximum straining obtained with same sequence as **b** shows an iliococcygeus angle (enclosed between the two dashed lines) of 71.0°.

Our study used phased-array coils in MR imaging in patients with anal incontinence. The different patterns and sites of injuries diagnosed in patients in group D in our study are comparable to those in previous reports (33,36). In group D patients with anal incontinence, static MR imaging showed no sphincter defect in two patients, whereas dynamic images revealed marked muscle weakness in all members of this group. Combined analysis of both types of MR images suggested that in the absence of an anal sphincter defect, anal incontinence could be associated with marked levator muscle weakness.

In contrast to other reported findings (2,14), we observed the width of the levator hiatus and the iliococcygeus angle to be statistically significant in the identification of pelvic floor laxity. Thus, we recommend that these measurements be added to the supporting measurements that have been found useful in the quantification of pelvic organ descent (14).

A limitation of our study was the heterogeneity of the patient groups. However, it was important to include patients with different clinical symptoms of pelvic dysfunction so that we could identify differences in the underlying anatomic derangement. For the

Figure 7

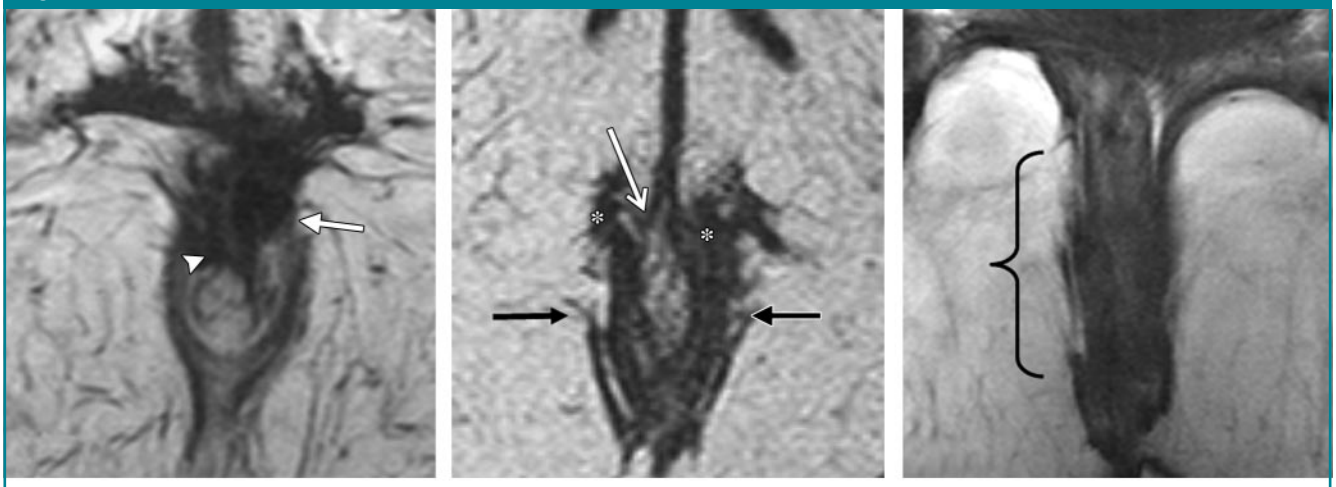

a. b. c.

Figure 7: Static MR images in two patients (one 54-year-old woman [**a**] and one 33-year-old woman [**b, c**]) with both anal incontinence and POP. **(a)** Axial balanced fast-field echo image (9/4) of anal sphincter complex. Arrow = scarring of external anal sphincter, arrowhead = scarring of internal anal sphincter. **(b)** Axial and **(c)** coronal MR images obtained with the same sequence as **a** show fraying and an anterior defect (*) of the internal anal sphincter with bulging mucosa (white arrow), plus a defect of the external anal sphincter (black arrows). The brace in **c** indicates a defect of the deep part of the external anal sphincter as well as the puborectalis muscle.

Table 5

Comparison of H-Line, M-Line, and Levator Plate Angle Measurements in Volunteer Subgroup A with Those in Volunteer Subgroup B and Patient Groups

Group Compared with Volunteer Subgroup A	H-Line			M-Line			Levator Plate Angle		
	t Value	*P* Value	95% CI (cm)	*t* Value	*P* Value	95% CI (cm)	*t* Value	*P* Value	95% CI (degrees)
Volunteer subgroup B	0.5488	.592	−1.585, 1.045	0.9289	.369	−2.326, 1.126	2.904	.0123	−40.994, 1.706
Patient group									
A	2.891	.010	−2.386, −0.094	2.895	.010	−1.630, 0.125	4.520	<.001	−46.095, −11.845
B	0.349	.730	−1.296, 0.996	1.918	.072	−2.584, 0.422	0.9720	.344	−23.355, 10.895
C	5.399	<.001	−3.139, −1.061	4.720	<.001	−3.774, −1.046	6.677	<.001	−54.340, −23.280
D	11.332	<.001	−6.352, −3.928	7.910	<.001	−6.301, −3.119	9.727	<.001	−84.040, −47.820

Note.—Measurements were obtained in the sagittal plane at maximum straining. CI = confidence interval.

Table 6

Comparison of Levator Hiatus and Iliococcygeus Angle Measurements in Volunteer Subgroup A with Those in Volunteer Subgroup B and Patient Groups

Group Compared with Volunteer Subgroup A	Width of Levator Hiatus in Axial Plane						Iliococcygeus Angle in Coronal Plane					
	At Rest			At Maximum Straining			At Rest			At Maximum Straining		
	t Value	*P* Value	95% CI (cm)	*t* Value	*P* Value	95% CI (cm)	*t* Value	*P* Value	95% CI (degrees)	*t* Value	*P* Value	95% CI (degrees)
Volunteer subgroup B	0.6292	.540	−0.4870, 0.7870	2.539	.055	−2.873, 0.07342	2.121	.059	−7.118, 0.8183	1.306	.214	−20.254, 6.954
Patient group												
A	4.427	.0004	−1.475, −0.364	5.679	<.001	−4.014, −1.446	2.433	.056	−6.609, 0.309	5.524	<.001	−36.380, −12.660
B	0.5293	.603	−0.44453, −0.665	0.291	.744	−1.144, 1.424	3.282	.004	−7.709, −0.790	0.545	.593	−14.280, 9.440
C	4.669	.0001	−1.384, −0.376	6.652	<.001	−4.065, −1.735	3.398	.002	−7.127, −0.852	6.849	<.001	−38.324, −16.815
D	5.550	.000056	−1.807, −0.632	6.786	<.001	−4.808, −2.092	4.835	.0002	−10.279, −2.961	8.464	<.001	−52.272, −27.188

Note.—CI = confidence interval.

same reason, the clinical data were made available to the radiologist who analyzed the images: to allow determination of whether combined analysis of both types of MR images could detect differences in the pathogenesis of these clinical problems and to determine whether analyzing both types of images together could provide all of the information necessary for diagnosis and relevant to treatment. We recognize that the utility of demonstrating the specific abnormality in the pelvic supporting structures in the management and treatment of pelvic floor dysfunction still must be validated, just as the reproducibility of our proposed analytic approach has to be determined. Nevertheless, it is worth mentioning that promising results have been reported with respect to the ability of imaging to change patient care in 41.6% (37), 41% (38), and 75% (39) of patients with different spectra of pelvic floor dysfunction.

In conclusion, combined analysis of both static and dynamic MR images in patients reporting SUI, POP, and anal incontinence provides complementary information and allows identification of certain structural abnormalities and their association with specific pelvic floor dysfunctions. This analytic approach gives insight into the diagnosis of these complex disorders and may also allow for a defect-specific approach to disease management and surgical technique.

Figure 8

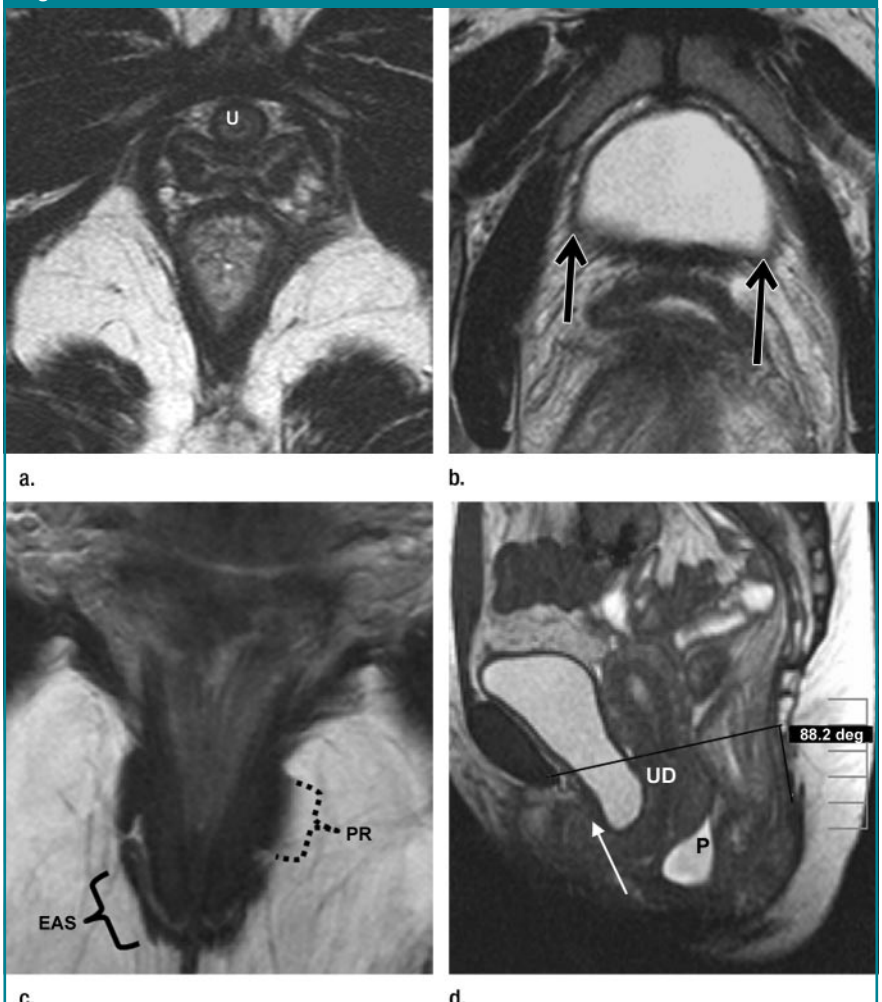

Figure 8: Static and dynamic MR images in 30-year-old patient with anal incontinence and POP but not SUI. **(a, b)** Static axial T2-weighted turbo spin-echo images (5000/132) show **(a)** normal urethral *(U)* supporting structures and **(b)** normal level I fascial support (arrows). **(c)** Static coronal balanced fast-field echo image (9/4) of anal sphincter shows no gross abnormality. *EAS* = external anal sphincter, *PR* = puborectalis muscle. **(d)** Dynamic sagittal balanced fast-field echo image (5/1.6) at maximum straining shows excessive levator plate sagging. The levator plate angle is 88.2°, indicating marked levator muscle weakness (arrow, bladder neck descent). *P* = peritoneocele, *UD* = uterine descent. Anterior repair of the puborectalis muscle and the peritoneocele and postanal repair of the levator hiatus were performed, without repair of the bladder neck. A normal anal sphincter was confirmed during surgery. At the 1-year follow-up examination, this patient did not report the appearance of masked SUI.

Acknowledgments: Special thanks to Professor Ahmed Samy, MD, PhD, and the professors in the Radiology Department at Cairo University Hospitals for providing R.F.E.S. the time and facilities needed to conduct research for this study; to Professor Tahany Elzainy, PhD, for assistance in organizing the information in the manuscript; to Amany Elbasmy, MD, PhD, who ensured the accuracy of our statistics; to Karen Kinkel, MD, PD, Jurgen Futterer, MD, PhD, Professor Jelle Barentsz, MD, PhD, and Professor Parvati Ramchandani, MD, for their efforts and their review of the manuscript; and to Katharine O'Moore-Klopf, BA, for editorial assistance.

References

1. Bump RC, Norton PA. Epidemiology and natural history of pelvic floor dysfunction. Obstet Gynecol Clin North Am 1998;25:723–746.
2. Singh K, Reid WM, Berger LA. Magnetic resonance imaging of normal levator ani anatomy and function. Obstet Gynecol 2002;99:433–438.
3. Klutke C, Golomb J, Barbaric Z, Raz S. The anatomy of stress incontinence: magnetic resonance imaging of the female bladder neck and urethra. J Urol 1990;143:563–566.
4. DeLancey JO. Fascial and muscular abnormalities in women with urethral hypermobility and anterior vaginal wall prolapse. Am J Obstet Gynecol 2002;187:93–98.
5. Stoker J, Rociu E, Bosch JL, et al. High-resolution endovaginal MR imaging in stress urinary incontinence. Eur Radiol 2003;13:2031–2037.
6. Kim JK, Kim YJ, Choo MS, Cho KS. The

urethra and its supporting structures in women with stress urinary incontinence: MR imaging using an endovaginal coil. AJR Am J Roentgenol 2003;180:1037–1044.

7. Huddleston HT, Dunnihoo DR, Huddleston PM, Meyers PC. Magnetic resonance imaging of defects in DeLancey's vaginal support levels I, II, and III. Am J Obstet Gynecol 1995;172:1778–1784.
8. Beets-Tan RG, Morren GL, Beets GL, et al. Measurement of anal sphincter muscles: endoanal US, endoanal MR imaging, or phased-array MR imaging? a study with healthy volunteers. Radiology 2001;220:81–89.
9. Laghi A, Iafrate F, Paolantonio P, et al. Magnetic resonance imaging of the anal canal using high resolution sequences and phased array coil: visualization of anal sphincter complex. Radiol Med (Torino) 2002;103: 353–359.
10. Yang A, Mostwin JL, Rosenshein NB, Zerhouni EA. Pelvic floor descent in women: dynamic evaluation with fast MR imaging and cinematic display. Radiology 1991;179: 25–33.
11. Comiter CV, Vasavada SP, Barbaric ZL, Gousse AE, Raz S. Grading pelvic prolapse and pelvic floor relaxation using dynamic magnetic resonance imaging. Urology 1999; 54:454–457.
12. Goh V, Halligan S, Kaplan G, Healy JC, Bartram CI. Dynamic MRI of the pelvic floor in asymptomatic subjects. AJR Am J Roentgenol 2000;174:661–666.
13. Kelvin FM, Maglinte DD, Hale DS, Benson JT. Female pelvic organ prolapse: a comparison of triphasic dynamic MR imaging and triphasic fluoroscopic cystocolpoproctography. AJR Am J Roentgenol 2000;174:81–88.
14. Fielding JR. Practical MR imaging of female pelvic floor weakness. RadioGraphics 2002; 22:295–304.
15. Kelvin FM, Pannu HK. Dynamic cystoproctography: fluoroscopic and MR techniques for evaluating pelvic organ prolapse. In: Bartram CI, DeLancey JO, Halligan S, Kelvin FM, Stoker J, eds. Imaging pelvic floor disorders. New York, NY: Springer, 2003; 51–68.
16. Pannu HK, Kaufman HS, Cundiff GW, et al. Dynamic MR imaging of pelvic organ prolapse: spectrum of abnormalities. RadioGraphics 2000;20:1567–1582.
17. Mengert WF. Mechanics of uterine support and position. Am J Obstet Gynecol 1936;31: 775–782.
18. DeLancey JO. Anatomic aspects of vaginal eversion after hysterectomy. Am J Obstet Gynecol 1992;166(6 pt 1):1717–1724.
19. DeLancey JO. Anatomy and biomechanics of genital prolapse. Clin Obstet Gynecol 1993; 36:897–909.
20. DeLancey JO. Functional anatomy of the pelvic floor. In: Bartram CI, DeLancey JO, Halligan S, Kelvin FM, Stoker J, eds. Imaging pelvic floor disorders. New York, NY: Springer, 2003; 27–38.
21. Jeffcoate TN, Roberts H. Observation on stress incontinence of urine. Am J Obstet Gynecol 1952;64:721–738.
22. Enhorning G. Simultaneous recording of intravesical and intra-urethral pressure: a study on urethral closure in normal and stress incontinent women. Acta Chir Scand Suppl 1961;276:1–69.
23. Mostwin JL, Yang A, Sanders R, Genadry R. Radiography, sonography, and magnetic resonance imaging for stress urinary incontinence: contributions, uses, and limitations. Urol Clin North Am 1995;22:539–549.
24. DeLancey JO. Structural support of the urethra as it relates to stress urinary incontinence: the hammock hypothesis. Am J Obstet Gynecol 1994;170:1713–1720.
25. DeLancey JO. Anatomy and physiology of urinary incontinence. Clin Obstet Gynecol 1990;33:298–307.
26. Olsen AL, Smith VJ, Bergstrom JO, Colling JC, Clark AL. Epidemiology of surgically managed pelvic organ prolapse and urinary incontinence. Obstet Gynecol 1997;89:501–506.
27. DeLancey JO. The hidden epidemic of pelvic floor dysfunction: achievable goals for improved prevention and treatment. Am J Obstet Gynecol 2005;192:1488–1495.
28. Petros PP. Appendix 1. Patient questionnaires and other diagnostic resource tools. In: The female pelvic floor: function, dysfunction and management according to the integral theory. New York, NY: Springer, 2004; 194–197.
29. Goodrich MA, Webb MI, King BF, et al. Magnetic resonance imaging of pelvic floor relaxation: dynamic analysis and evaluation of patients before and after surgical repair. Obstet Gynecol 1993;82:883–891.
30. Pescatori M, Anastasio G, Bottini C, Mentasti A. New grading system and scoring for anal incontinence: evaluation of 335 patients. Dis Colon Rectum 1992;35:482–487.
31. Theofrastous JP, Swift SE. The clinical evaluation of pelvic floor dysfunction. Obstet Gynecol Clin North Am 1998;25:783–804.
32. El Sayed RF, Morsy MM, El-Mashed SM, Abdel-Azim MS. Anatomy of the urethral supporting ligaments defined by dissection, histology, and MRI of female cadavers and MRI of healthy nulliparous women. AJR Am J Roentgenol 2007;189:1145–1157.
33. Rociu E, Stoker J, Zwamborn AW, Laméris JS. Endoanal MR imaging of the anal sphincter in fecal incontinence. RadioGraphics 1999;19(spec no):S171–S177.
34. Bergman A, Elia G. Three surgical procedures for genuine stress urinary incontinence: 5-year follow-up of a prospective randomized study. Am J Obstet Gynecol 1995;173:66–71.
35. Horbach N. Choosing the appropriate surgery for genuine stress urinary incontinence. Oper Tech Gynecol Surg 1997;2:1–4.
36. Terra MP, Beets-Tan RH, van Der Hulst VP, et al. Anal sphincter defects in patients with fecal incontinence: endoanal versus external phased-array MR imaging. Radiology 2005; 236:886–895.
37. El Sayed RF, Fielding JR, El Mashed S, Morsy MM, Abd El Azim MS. Preoperative and postoperative magnetic resonance imaging of female pelvic floor dysfunction: correlation with clinical findings. J Womens Imaging 2005;7:163–180.
38. Kaufman HS, Buller JL, Thompson JR, et al. Dynamic pelvic magnetic resonance imaging and cystocolpoproctography alter surgical management of pelvic floor disorders. Dis Colon Rectum 2001;44:1575–1584.
39. Altringer WE, Saclarides TJ, Dominguez JM, Brubaker LT, Smith CS. Four-contrast defecography: pelvic "floor-oscopy." Dis Colon Rectum 1995;38:695–699.

Radiology 2008

This is your reprint order form or pro forma invoice

(Please keep a copy of this document for your records.)

Reprint order forms and purchase orders or prepayments must be received 72 hours after receipt of form either by mail or by fax at 410-820-9765. It is the policy of Cadmus Reprints to issue one invoice per order. **Please print clearly**.

Author Name _____
Title of Article _____
Issue of Journal_____ Reprint # _____ Publication Date _____
Number of Pages_____ KB # _____ Symbol Radiology
Color in Article? Yes / No (Please Circle)

Please include the journal name and reprint number or manuscript number on your purchase order or other correspondence.

Order and Shipping Information

Reprint Costs **(Please see page 2 of 2 for reprint costs/fees.)**

_____ Number of reprints ordered $_____
_____ Number of color reprints ordered $_____
_____ Number of covers ordered $_____
Subtotal $_____
Taxes $_____

(*Add appropriate sales tax for Virginia, Maryland, Pennsylvania, and the District of Columbia or Canadian GST to the reprints if your order is to be shipped to these locations*.)

First address included, add $32 for each additional shipping address $_____

TOTAL $_____

Shipping Address **(cannot ship to a P.O. Box) Please Print Clearly**

Name _____
Institution _____
Street _____
City _____ State _____ Zip _____
Country _____
Quantity_____ Fax _____
Phone: Day _____ Evening _____
E-mail Address _____

Additional Shipping Address* **(cannot ship to a P.O. Box)**

Name _____
Institution _____
Street _____
City _____ State _____ Zip _____
Country _____
Quantity _____ Fax _____
Phone: Day _____ Evening _____
E-mail Address _____
** Add $32 for each additional shipping address*

Payment and Credit Card Details

Enclosed: Personal Check _____
Credit Card Payment Details _____
Checks must be paid in U.S. dollars and drawn on a U.S. Bank.

Credit Card: __ VISA __ Am. Exp. __ MasterCard
Card Number _____
Expiration Date_____
Signature: _____

Please send your order form and prepayment made payable to:

Cadmus Reprints
P.O. Box 751903
Charlotte, NC 28275-1903

Note: Do not send express packages to this location, PO Box.
FEIN #:541274108

Invoice or Credit Card Information

Invoice Address Please Print Clearly
Please complete Invoice address as it appears on credit card statement

Name _____
Institution _____
Department _____
Street _____
City _____ State _____ Zip _____
Country _____
Phone _____ Fax _____
E-mail Address _____

Cadmus will process credit cards and *Cadmus Journal Services* will appear on the credit card statement.

If you don't mail your order form, you may fax it to 410-820-9765 with your credit card information.

Signature _____ Date _____
Signature is required. By signing this form, the author agrees to accept the responsibility for the payment of reprints and/or all charges described in this document.

RB-9/26/07

Radiology 2008

Black and White Reprint Prices

Domestic (USA only)						
# of Pages	50	100	200	300	400	500
1-4	$221	$233	$268	$285	$303	$323
5-8	$355	$382	$432	$466	$510	$544
9-12	$466	$513	$595	$652	$714	$775
13-16	$576	$640	$749	$830	$912	$995
17-20	$694	$775	$906	$1,017	$1,117	$1,220
21-24	$809	$906	$1,071	$1,200	$1,321	$1,471
25-28	$928	$1,041	$1,242	$1,390	$1,544	$1,688
29-32	$1,042	$1,178	$1,403	$1,568	$1,751	$1,924
Covers	$97	$118	$215	$323	$442	$555

International (includes Canada and Mexico)						
# of Pages	50	100	200	300	400	500
1-4	$272	$283	$340	$397	$446	$506
5-8	$428	$455	$576	$675	$784	$884
9-12	$580	$626	$805	$964	$1,115	$1,278
13-16	$724	$786	$1,023	$1,232	$1,445	$1,652
17-20	$878	$958	$1,246	$1,520	$1,774	$2,030
21-24	$1,022	$1,119	$1,474	$1,795	$2,108	$2,426
25-28	$1,176	$1,291	$1,700	$2,070	$2,450	$2,813
29-32	$1,316	$1,452	$1,936	$2,355	$2,784	$3,209
Covers	$156	$176	$335	$525	$716	$905

Color Reprint Prices

Domestic (USA only)						
# of Pages	50	100	200	300	400	500
1-4	$223	$239	$352	$473	$597	$719
5-8	$349	$401	$601	$849	$1,099	$1,349
9-12	$486	$517	$852	$1,232	$1,609	$1,992
13-16	$615	$651	$1,105	$1,609	$2,117	$2,624
17-20	$759	$787	$1,357	$1,997	$2,626	$3,260
21-24	$897	$924	$1,611	$2,376	$3,135	$3,905
25-28	$1,033	$1,071	$1,873	$2,757	$3,650	$4,536
29-32	$1,175	$1,208	$2,122	$3,138	$4,162	$5,180
Covers	$97	$118	$215	$323	$442	$555

International (includes Canada and Mexico))						
# of Pages	50	100	200	300	400	500
1-4	$278	$290	$424	$586	$741	$904
5-8	$429	$472	$746	$1,058	$1,374	$1,690
9-12	$604	$629	$1,061	$1,545	$2,011	$2,494
13-16	$766	$797	$1,378	$2,013	$2,647	$3,280
17-20	$945	$972	$1,698	$2,499	$3,282	$4,069
21-24	$1,110	$1,139	$2,015	$2,970	$3,921	$4,873
25-28	$1,290	$1,321	$2,333	$3,437	$4,556	$5,661
29-32	$1,455	$1,482	$2,652	$3,924	$5,193	$6,462
Covers	$156	$176	$335	$525	$716	$905

Minimum order is 50 copies. For orders larger than 500 copies, please consult Cadmus Reprints at 800-407-9190.

Reprint Cover

Cover prices are listed above. The cover will include the publication title, article title, and author name in black.

Shipping

Shipping costs are included in the reprint prices. Domestic orders are shipped via UPS Ground service. Foreign orders are shipped via a proof of delivery air service.

Multiple Shipments

Orders can be shipped to more than one location. Please be aware that it will cost $32 for each additional location.

Delivery

Your order will be shipped within 2 weeks of the journal print date. Allow extra time for delivery.

Tax Due

Residents of Virginia, Maryland, Pennsylvania, and the District of Columbia are required to add the appropriate sales tax to each reprint order. For orders shipped to Canada, please add 7% Canadian GST unless exemption is claimed.

Ordering

Reprint order forms and purchase order or prepayment is required to process your order. Please reference journal name and reprint number or manuscript number on any correspondence. You may use the reverse side of this form as a proforma invoice. Please return your order form and prepayment to:

Cadmus Reprints
P.O. Box 751903
Charlotte, NC 28275-1903

Note: Do not send express packages to this location, PO Box.
FEIN #:541274108

Please direct all inquiries to:

Rose A. Baynard
800-407-9190 (toll free number)
410-819-3966 (direct number)
410-820-9765 (FAX number)
baynardr@cadmus.com (e-mail)

Reprint Order Forms and purchase order or prepayments must be received 72 hours after receipt of form.